International Journal of the Korean Society of Precision Engineering, Vol. 4, No. 3, May 2003

A Model of Magnetic Bearings Considering Eddy Currents and Hysteresis

Myounggyu Noh[1, #]

[1] Department of Mechatronics Engineering, Chungnam National University, Daejeon, South Korea

ABSTRACT

A simulation model for radial magnetic bearings is presented. The model incorporates hysteresis, saturation and eddy current effects. A simple magnetization model that describes hysteresis and saturation is proposed. Eddy currents are taken into consideration by assuming that they are generated by single-turn fictitious coils wrapped around each magnetic flux path. The dynamic equations describing the simulation model can easily incorporate the operation of switching power amplifier. A simulation of a typical 8-pole radial magnetic bearing produces switching waveforms very similar to the experimental observation.

Key Words : Magnetic bearing, Magnetic circuit model, Hysteresis, Eddy currents

Nomenclature

H	Magnetic field intensity (A/m)
B	Magnetic flux density (T)
μ_0	Permeability of free space = $4\pi \times 10^{-7}$ H/m
μ_r	Relative permeability
ϕ	Magnetic flux (Wb)
δ	Skin depth (m)
n	Coil turns
V	Voltage
r	Resistance of coil
A	Pole face area
i	Coil currents

1. Introduction

When a magnetic bearing design is evaluated, an idealized linear magnetic model based on magnetic circuit theory is usually used while neglecting such effects as saturation, hysteresis and eddy currents. However, this idealized model becomes less accurate if the bearing is required to operate in conditions where the effects of hysteresis, saturation and eddy currents cannot be ignored. A good example of such a case would be self-sensing magnetic bearings where the journal position is estimated by the switching waveforms of the coil currents and the voltages applied to them[1,2]. The non-ideal effects such as hysteresis and eddy currents can significantly influence the performance of the bearing as a sensor in terms of sensitivity and repeatability.

In this paper, a simulation model of a radial magnetic bearing is presented. This model includes the effects of saturation and hysteresis of the bearing material. The simulation model also takes into consideration the effect of eddy currents generated in the flux path by the time-varying magnetic fields.

The material nonlinearities such as saturation and hysteresis are described by a set of algebraic equations heuristically developed from the experimental magnetization curve. This is in contrast to the work by Springer, *et. al.* [3], where they used a more complex and computationally taxing magnetization model. The effects of eddy currents are modeled by simply assuming that the eddy currents are generated by single-turn fictitious coils wrapped around each magnetic path. The

Corresponding Author :
Email : mnoh@cnu.ac.kr
Tel.+82-42-821-6877

simulation model does not assume the type of amplifier driving the bearing. Therefore, it is easy to deal with switching amplifiers commonly used in magnetic bearing systems.

The simulation model produces the switching waveforms very similar to those obtained experimentally, which is essential in evaluating the performance of self-sensing algorithms based on the switching waveform.

The structure of the paper is as follows. Immediately following the introduction are the descriptions of the model of nonlinear magnetic properties and the eddy current effects. Section 3 contains the development of the modified magnetic circuit models for a single-pole actuator and an 8-pole radial magnetic bearing, which include hysteresis, saturation and eddy current effects, followed by some simulation results and observations.

2. Magnetic Properties of Material

2.1 Hysteresis and Saturation Model

The literature contains numerous models of the magnetic hysteresis phenomenon. These models are derived either on the basis of mathematical description of the hysteresis[4], or magnetic domain theory[5]. Although these models are capable of describing complex magnetization process, they are usually given as differential equations or integral equations. Therefore, the nonlinearity only becomes obvious after solving the equations either analytically or numerically. This complexity makes it difficult to employ these models for the purpose of assessing the effects of magnetic nonlinearity on the performance of the bearing.

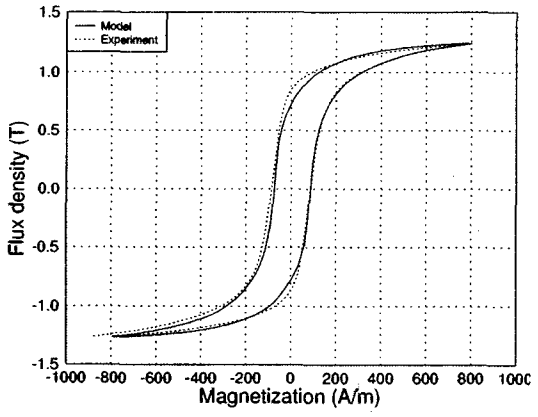

Fig. 1 Simulated magnetization curve compared with experimental data of silicon iron

In this paper, a rather simple magnetization model is used. This model is given as an algebraic equation, which can be conveniently employed into the bearing model. The magnetization model used in this paper assumes that the magnetization curve is confined by two envelopes represented by

$$H_1(B) = \frac{B}{\mu_0 \mu_r^0} + \frac{\sigma}{\mu_0}\left(1 - \frac{1}{\mu_r^0}\right)\log[1 + \eta \cdot e^{(B - B_s)/\sigma}] + H_c \quad (1)$$

$$H_2(B) = \frac{B}{\mu_0 \mu_r^0} - \frac{\sigma}{\mu_0}\left(1 - \frac{1}{\mu_r^0}\right)\log[1 + \eta \cdot e^{(-B - B_s)/\sigma}] - H_c \quad (2)$$

where B is the flux density and H is the magnetic field intensity. The parameters μ_r^0 , σ , η , B_s , H_c are determined from the experimental magnetization curve. The actual magnetization H as a function of flux density B is given by

$$H(B) = \begin{cases} H_1(B) - [H_1(B_o) - H(B_o)] \cdot e^{-\beta \mid B - B_o \mid} & \text{if } \dot{B} \geq 0 \\ H_2(B) - [H_2(B_o) - H(B_o)] \cdot e^{-\beta \mid B - B_o \mid} & \text{if } \dot{B} < 0 \end{cases} \quad (3)$$

where B_o is the flux density at the instant that $\dot{B}$ changes its sign. The parameter β determines the shape of the actual magnetization curve. A smaller β represents soft magnetic material, whereas a larger β describes hard magnetic material.

The parameters that define the magnetization model can be obtained by curve-fitting the simulated B-H curve with the experimental data. Various optimization techniques can be used for this purpose. In this paper, a simplex method is employed. Using the experimental B-H curve for silicon iron, the following parameters were identified from the simplex search:

μ_r^0	50942	
η	0.00474	
σ	0.17579	tesla
B_s	1.25	tesla
β	8.2	tesla^{-1}
H_c	81.35	ampere-turns/meter

Figure 1 shows the magnetization model for silicon iron (solid line) compared with the experimental data (dotted line).

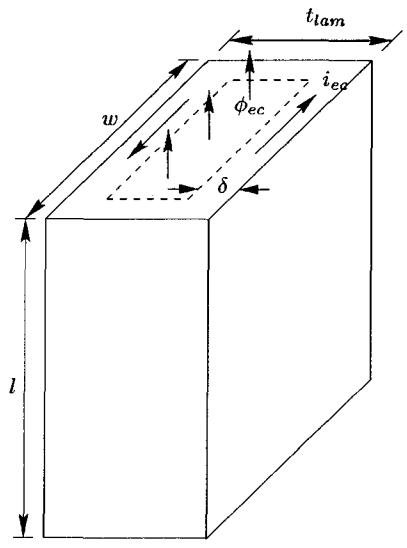

Fig. 2 Modeling of eddy currents in a lamination of a pole-piece

2.2 Eddy Current Model

The effects of eddy currents can be modeled in several ways. One approach would be to use rate-dependent permeability for the stator material[6]. In this paper, it is assumed that eddy currents are generated from single-turn fictitious coils wrapped around the flux paths[7] (see Fig. 2). The accuracy of this model depends on the correct estimation of the amount of flux linked by this eddy current loop and its electrical resistance seen by the eddy current loop. Since each eddy current loop stays within a given lamination of the core, it is reasonable to assume that the total flux linked by the fictitious coils would reduce by the ratio between the thickness of the lamination and the thickness of the lamination stack. However, this ratio overestimates the driving flux because the eddy currents are not perfectly concentrated on the surface. Assuming the eddy currents are uniformly distributed throughout a characteristic skin depth d, the flux linked would be

$$\phi_{ec} = \left(\frac{t_{lam} - \delta}{t_{stack}}\right)\phi = \alpha\phi \tag{4}$$

where α is the scale factor.

The resistance seen by the eddy currents is roughly the stator resistivity, ρ, times the mean current path length divided by the area. For a pole of length l parallel

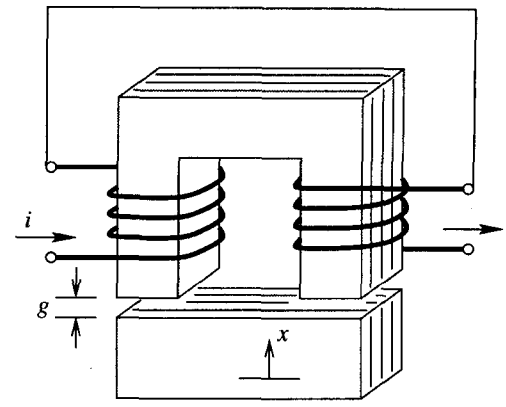

Fig. 3 Schematic of a single-pole actuator

to the flux and width w perpendicular to the flux and to the lamination direction, the resistance would be approximated by

$$r_{ec} = \frac{2\rho w}{l\delta} \tag{5}$$

3. Simulation Model

3.1 Simulation Model for a Single-Pole Actuator

Although it is much simpler than a typical magnetic bearing, a simulation model for a single-pole magnetic actuator suffices to analytically show the effects of hysteresis and eddy currents. The governing laws that relate the voltage and currents are the Faraday's induction law and the Ampere's loop law. The material constitutive law defines the relationship between the magnetization and the resulting magnetic flux. Combining the governing equations with the magnetization model and the eddy currents effects described above, we can obtain the following simulation model that relates the coil voltage V and the coil current i [8].

$$\dot{\phi} = \frac{nr_{ec}}{2n^2r_{ec} + 4\alpha r} \cdot V - \frac{rr_{ec}}{2n^2r_{ec} + 4\alpha r}(l_cH_c + 2gH_g) \tag{6}$$

$$i = \frac{2\alpha}{2n^2r_{ec} + 4\alpha r} \cdot V + \frac{nr_{ec}}{2n^2r_{ec} + 4\alpha r}(l_cH_c + 2gH_g) \tag{7}$$

where l_c is the core length and g is the air gap length. The magnetic field intensity H_c in the core is related to the magnetic flux through the magnetization model given in the previous section as

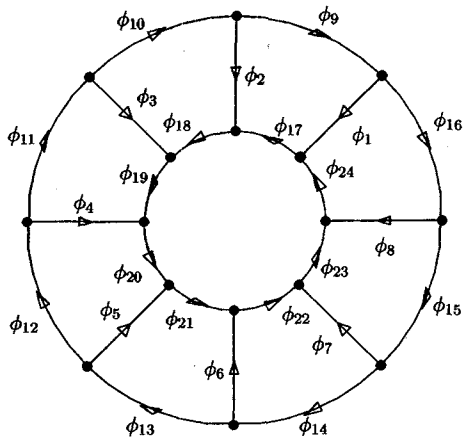

Fig. 4 Magnetic flux paths in an 8-pole radial magnetic bearing

$$H_c = \mathrm{H}(\phi) = \frac{\phi}{\mu_0 \mu_r(\phi) A} \tag{8}$$

The field intensity H_g in the air gap is linearly related to the flux as

$$H_g = \frac{\phi}{\mu_0 A} \tag{9}$$

If there is no eddy currents in the core, the resistance r_{ec} goes infinite, and equations (6) and (7) becomes the conventional voltage-current relationship for a single-pole actuator:

$$V = L\frac{di}{dt} + ri \tag{10}$$

where L is the inductance of the coil.

3.2 Simulation Model for a 8-Pole Magnetic Bearing

The previous simulation model for the single-pole actuator can be extended to an 8-pole radial bearing configuration, which is the most popular actuator type of magnetic bearings. Referring to Fig. 4 that shows all the flux paths of an 8-pole radial bearing, the Faraday's law to the two adjacent coils wired in series can be written as

$$n\frac{d\phi_{2i-1}}{dt} - n\frac{d\phi_{2i}}{dt} = V_i - 2ri_i, \quad i = 1,\ldots,4 \tag{11}$$

where n is the number of coil turns in each pole and r is the resistance of the each coil. This equation assumes that all eight coils have identical number of turns and coil resistance.

Assuming that fictitious single-turn coils wrapped around the flux paths produce eddy currents, Faraday's law for these fictitious coils can be written

$$\alpha\frac{d\phi_i}{dt} = -r_{ec}i_{ec_i}, \qquad i = 1,\ldots,24 \tag{12}$$

where α is defined in eq. (4). The above two equations can be written as one matrix equation.

$$\begin{bmatrix} W^T N \\ \alpha I \end{bmatrix}\frac{d\phi}{dt} = BV - \begin{bmatrix} W^T R W & \mathbf{0}_{4\times 24} \\ \mathbf{0}_{24\times 4} & R_{ec} \end{bmatrix} i \tag{13}$$

in which W is the interconnection matrix and R_{ec} is the eddy current resistance matrix.

The vector ϕ in (13) has 24 elements, which can be reduced to 9 using the conservation of flux. Following the numbering scheme illustrated in Fig. 4, conservation of flux produces 15 equations:

$$\begin{aligned} \phi_k + \phi_{k+7} - \phi_{k+8} &= 0, \qquad k = 2,\ldots,8 \\ \phi_k + \phi_{k+15} - \phi_{k+16} &= 0, \qquad k = 2,\ldots,8 \\ \phi_1 + \phi_2 + \cdots + \phi_8 &= 0 \end{aligned}$$

Or in matrix form,

$$C\phi = 0 \tag{14}$$

Eq. (14) means that the flux vector ϕ is in the null space of C. Then we can define $\hat{\phi}$ such that

$$\phi = C_\perp^T \hat{\phi} \tag{15}$$

where $C_\perp$ is the orthogonal complement of C [9]. Given the flux vector ϕ, the magnetization vector H can be determined from the constitutive law. As stated in the single-pole actuator case, the constitutive law can be written as

$$H = \mathrm{H}(\phi) \tag{16}$$

whether the magnetic material is linear or nonlinear.

The magnetization vector H is related to the coil currents and eddy currents and the Ampere's loop law can describe this relationship. In matrix form, the loop law can be expressed as[10]

$$LH + GH_g = Si \tag{17}$$

Combining the above governing equations, we can obtain the dynamic model of the magnetic bearing. Referring to the work by Noh *et. al.*[10] that contains the detailed derivation, the dynamic model of a radial magnetic bearing can be written as

$$\dot{\phi} = P(LH + GH_g) + QV \tag{18}$$

$$i = D(LH + GH_g) + EV \tag{19}$$

The matrices P, Q, D, E in (18) and (19) are defined as

$$P = K\mathbf{W}[S_\perp^T(K_\perp \mathbf{W} S_\perp^T)^{-1}K_\perp \mathbf{W} - I]S^T(SS^T)^{-1}$$
$$Q = K[I - \mathbf{W}S_\perp^T(K_\perp \mathbf{W} S_\perp^T)^{-1}K_\perp]B$$
$$D = [I - S_\perp^T(K_\perp \mathbf{W} S_\perp^T)^{-1}K_\perp \mathbf{W}]S^T(SS^T)^{-1}$$
$$E = S_\perp^T(K_\perp \mathbf{W} S_\perp^T)^{-1}K_\perp B$$

In the matrix definitions above, the matrix K is defined as

$$K = \left(\begin{bmatrix} W^T N \\ \alpha I \end{bmatrix} C_\perp^T \right)^\dagger$$

where $\dagger$ means the pseudo-inverse[8], and

$$\mathbf{W} = \begin{bmatrix} W^T R W & 0 \\ 0 & R_{ec} \end{bmatrix}$$

Using equations (18) and (19), we can investigate the magnetic fluxes in all of the paths and the coil currents resulting from the application of the voltages. It is worth noting here that the simulation model assumes nothing of the voltage input generated from the power amplifier. Therefore, the dynamic model can easily deal with the use of switching power amplifier, common amplifier type in industrial applications.

4. Results

An eight pole radial magnetic actuator made of silicon iron is selected to test the simulation model developed in the previous sections. Table 1 lists the critical dimensions of the test bearing. The eight poles of the test bearing are each of equal proportions and are spaced evenly around the circular journal.

Given the selected geometry and magnetic materials, three important operating parameters needs to be selected. These are the nominal bias current, the power supply voltage, and the effective eddy current skin depth. The first two can be chosen in a very straightforward manner. Noting that the silicon iron begins to saturate at a current of about 6 amperes, the bias current was set at 2 amperes to provide enough slew rate and linear operating range. The amplifier voltage was adjusted to 70 volts, which provides adequate dynamic performance and generates the switching ripple to be about 10% of the bias current.

The selection of the skin depth is less apparent than the other two parameters. Clearly, the skin depth cannot exceed one half of the lamination thickness and it is expected to diminish in thickness with increased switching frequency. By comparing the simulated current waveforms with experimental data, the skin depth was estimated to be about 10% of the lamination thickness.

With the bearing geometry and parameters described

Table 1 Geometry of test bearing

Stator outer diameter	119.1 mm
Backiron radial thickness	7.62 mm
Pole width	7.62 mm
Pole length	30.48 mm
Lamination thickness	0.178 mm
Stack thickness	10.16 mm
Shaft diameter	25.4 mm
Air gap	0.127 mm
Number of turns per pole	70

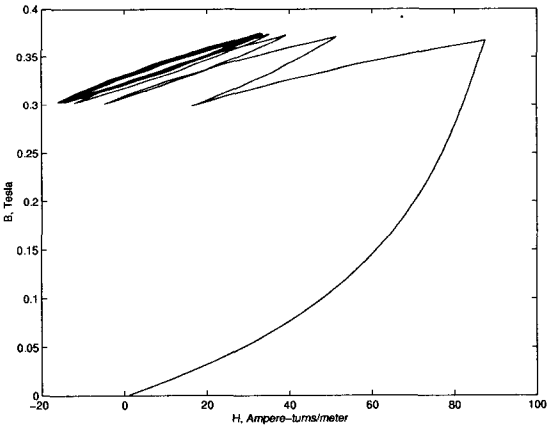

Fig. 5 Field intensity H versus flux density B

above, a simulation is performed when the coil currents increase from zero to the bias point. Figure 5 shows the transient behavior of flux density versus field intensity. The simulation results clearly indicate that the B-H curve converges to a stable minor hysteresis loop. This means that the switching amplifier causes the field to converge to a stable and repeatable loop on the B-H curve so that the average B-H relationship would be expected to show no hysteresis. Therefore, hysteresis would not affect DC force estimates obtained from the current with no hysteresis model. Note that this apparent stability may be an artifact of the model, but it should be emphasized that no particular effort was made in developing the model to produce this result. Although physically reasonable, this convergence to a stable minor loop must be verified by experiments.

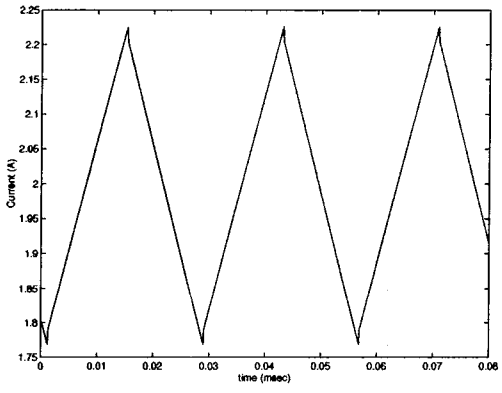

Fig. 6 Simulated current waveform

Figure 6 shows the time transients of current signals produced by the simulation model. The results demonstrate the discontinuity due to eddy current effects at the transition of voltage polarity. This discontinuity is consistent with the experimentally observed current waveform, which was measured from the test bearing. Figure 7 shows the actual current waveform in the coil. The reason that the overall amplitude of the measured waveform is smaller than that of the simulation seems to be due to the leakage and fringing effects. Leakage and fringing increases coil inductance, which results in smaller current ripple than expected. This paper does not consider these leakage and fringing effects, but the simulation model can incorporate these effects by, for example, adding leakage and fringing paths[6].

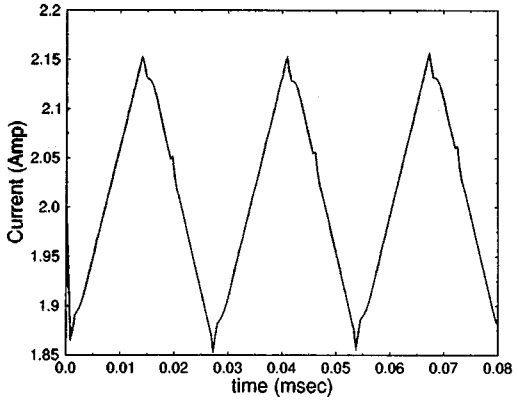

Fig. 7 Experimentally measured current waveform

5. Conclusion

In this paper, we presented a simulation model for radial magnetic bearings that included the effects of saturation, hysteresis, and eddy currents. The simulation model was derived without making assumptions on power amplifiers. Thus, a switching amplifier could easily be handled. The simulation results showed that the model correctly predicted the minor hysteresis loop to which the magnetization curve converges and the discontinuity in the current switching waveforms due to eddy current effects. This discontinuity was also verified with experiments.

Using this simulation model, it would be possible to see the effects of hysteresis and eddy currents on the performance of magnetic bearings operating in severe conditions. Also, a parametric study can be carried out to assess the accuracy of self-sensing magnetic bearings due to eddy currents and hysteresis in various working conditions.

Acknowledgement

This research was supported by Korea Research Foundation Grant (KRF-2000-003-E00041). The author would like to thank their general support.

References

1. Noh, M. and Maslen, E. H., "Self-Sensing Active Magnetic Bearings Based on Parameter Estimation," IEEE Transactions on Instrumentation and

Measurement, Vol. 46, No. 1, pp. 45-50, 1997.
2. Okada, Y., Mastuda, K., Nagai, B., "Sensorless Magnetic Levitation Control by Measuring the PWM Carrier Frequency Component," Proc. ISMB3, Alexandria, U.S.A., 1992.
3. Springer, H., Schlager, G., Platter, T., "A Nonlinear Simulation Model for Active Magnetic Bearing Actuators," Proc. ISMB6, Cambridge, U.S.A, 1998.
4. Hodgdon, M., "Applications of a Theory of Ferromagnetic Hysteresis," IEEE Transactions on Magnetics, Vol. 24, pp. 218-221, 1988.
5. Jiles, D. and Atherton, D., "Theory of Ferromagnetic Hysteresis," Journal of Magnetism and Magnetic Materials, Vol. 61, pp. 48-60, 1986.
6. Meeker, D. C., Maslen, E. H., Noh, M., "An Augmented Circuit Model for Magnetic Bearings Including Eddy Currents, Fringing, and Leakage," IEEE Transactions on Magnetics, Vol. 32, No. 4, pp. 3219-3227, 1996.
7. Noh, M., "Self-sensing Active Magnetic Bearings Driven by a Switching Power Amplifier," Ph.D. Thesis, University of Virginia, 1996.
8. Noh, M. and Jeong, M. K., "The Effects of Eddy Currents and Hysteresis on the Performance of Inductive Position Sensor for Magnetic Bearings," KSME Spring Conference, Jeju Island, 2001.
9. J. Ortega, Matrix Theory, Plenum Press, 1987.
10. Noh, M., Montie, D., Maslen, E. H. and Kondoleon, A., "A Simulation Model for the Analysis of Transient Magnetic Bearing Performance," Proceedings of 7th International Symposium on Magnetic Bearings, Zurich, 2000.